

# Numerical Analysis of Fixed Bed Adsorption Kinetics Using Orthogonal Collocation

In-Soo Park<sup>†</sup>

School of Chemical Engineering, Kyungnam University, Masan 631-701, Korea  
(Received 8 June 2002 • accepted 1 October 2002)

**Abstract**—Fixed bed adsorption kinetics is analyzed to test the validity of the simplified model based on the linear driving force approximation by comparison with the exact model by using the orthogonal collocation method. The axial dispersion, the external film diffusion, and the intraparticle diffusion are considered to be the major mass transfer phenomena involved with the fixed bed adsorption kinetics in this study. It is assumed that a local equilibrium is attained at the fluid-solid interface and the equilibrium can be described by the Langmuir isotherm. A homogeneous particle diffusion model is employed to describe the intraparticle diffusion.

Key words: Adsorption, Fixed Bed, Breakthrough Curve, Orthogonal Collocation, Linear Driving Force Approximation

## INTRODUCTION

Various mass transfer phenomena are involved with fixed bed adsorption kinetics: axial dispersion, external diffusion, adsorption on the fluid-particle interface, and intraparticle diffusion. For systems with nonlinear adsorption isotherm, it is difficult to obtain an exact analytical solution for the breakthrough curve at the exit of the adsorption bed. Thus, the design and modeling of the fixed bed adsorption kinetics, especially in case of systems with nonlinear isotherm, requires numerical computations of a mathematical model.

For the numerical solution of the model, the finite difference [Crittenden and Weber, Jr., 1978; Yun, 2000], the orthogonal collocation [Raghavan and Ruthven, 1983; Xiu and Li, 2000], and the combined orthogonal collocation (along the particle radius) and finite difference (along the bed) [Chatzopoulos and Varma, 1995] have been adopted. It is commonly known that orthogonal collocation has difficulty in describing steep concentration profiles. However, for a relatively smooth concentration profile, orthogonal collocation is preferred over finite difference because of the greater stability and less computation time of the former [Raghavan and Ruthven, 1983].

A rigorous numerical solution of the fixed bed adsorption kinetics is quite time-consuming, since it has to account for temporal evolution as well as multivariable spatial distribution of adsorbate concentration. However, the computational effort can be greatly reduced if we replace the original intraparticle diffusion equation by the linear driving force (LDF) approximation [Moon et al., 1992; Lee and Moon, 2001; Kim et al., 2002], which was originally proposed by Gluckauf and Coates [1947].

In this study, we will test the validities of several simplified models based on the LDF approximation by comparison with the exact model. We will adopt orthogonal collocation in the numerical computation. All the computations in the present study will be carried out by using the MATLAB programming language.

## MATHEMATICAL MODEL

We consider an isothermal bed packed with porous spherical par-

ticles. Initially an inert material flows through the bed. At time zero, a step amount of adsorbing species is introduced to the inlet of the bed. As the adsorbing species flows through the bed, the axial dispersion, the external film diffusion, and the intraparticle diffusion of the adsorbing species take place.

The mass balance in the bed is

$$\frac{\partial C_b}{\partial t} = \frac{D_L}{\epsilon_b} \frac{\partial^2 C_b}{\partial z^2} - v \frac{\partial C_b}{\partial z} - \left( \frac{1 - \epsilon_b}{\epsilon_b} \right) \left( \frac{3k_f}{R} \right) (C_b - C_s) \quad (1a)$$

where  $C_b$  is the concentration in the fluid phase,  $C_s$  is the concentration in the fluid phase at the surface of a particle,  $R$  is the characteristic length of the particle,  $D_L$  is the axial dispersion coefficient,  $\epsilon_b$  is the void fraction of the bed,  $v$  is the interstitial velocity through the bed, and  $k_f$  is the external mass transfer coefficient.

The initial and boundary conditions for Eq. (1a) are

$$\text{at } t=0, C_b=0 \quad (1b)$$

$$\text{at } z=0, \left[ \frac{D_L}{\epsilon_b} \frac{\partial C_b}{\partial z} \right]_{z=0} = -v(C_b|_{z=0} - C_0) = -v(C_0 - C_b|_{z=0}) \quad (1c)$$

$$\text{at } z=L, \frac{\partial C_b}{\partial z} = 0 \quad (1d)$$

where  $C_0$  is the magnitude of the step amount introduced to the inlet of the bed at time zero. Eqs. (1c) and (1d) are the Danckwerts boundary conditions, which are correct for a dispersed plug-flow system as discussed by Wehner and Wilhelm [1956].

To describe the mass transfer phenomena in the particle, we will employ a homogeneous particle diffusion model that accounts for the external-film diffusion followed by the surface diffusion in the particle. Other models (e.g., dual diffusion model of pore and surface diffusion in the particle) could be solved in exactly the same way. We assume that a local equilibrium is attained between the fluid phase and particle phase concentrations at the particle surface, and the equilibrium can be described by the Langmuir isotherm.

The mass balance equation (for the homogeneous particle diffusion model) describing the distribution of concentration inside the particle is:

$$\frac{\partial C_\mu}{\partial t} = \frac{1}{r^2} \frac{\partial}{\partial r} \left( r^2 D_e \frac{\partial C_\mu}{\partial r} \right) = D_e \left( \frac{\partial^2 C_\mu}{\partial r^2} + \frac{2}{r} \frac{\partial C_\mu}{\partial r} \right) \quad (2a)$$

where  $C_\mu$  is the concentration in the particle phase and  $D_e$  is the ef-

<sup>†</sup>To whom correspondence should be addressed.

E-mail: ispark@kyungnam.ac.kr

fective diffusivity, which is assumed constant in the present study.

The initial and boundary conditions are

$$\text{at } t=0, \quad C_\mu=0 \tag{2b}$$

$$\text{at } r=0, \quad \frac{\partial C_\mu}{\partial r}=0 \tag{2c}$$

$$\text{at } r=R, \quad \left[ D_e \frac{\partial C_\mu}{\partial r} \right]_{r=R} = k_f (C_b - C_s) \tag{2d}$$

where  $C_s$  is the concentration in the fluid phase at the surface of the particle.

Equilibrium at the particle surface is:

$$C_\mu|_{r=R} = \frac{C_{\mu s} b C_s}{1 + b C_s} \tag{3}$$

where  $C_{\mu s}$  and  $b$  are the Langmuir isotherm parameters.

The problem defined by Eqs. (1) and (2) is identical to the problem solved numerically by Raghavan and Ruthven [1983] who employed a linear isotherm instead of the Langmuir isotherm of Eq. (3). Note that the Langmuir isotherm of Eq. (3) reduces to a linear isotherm when the value of the adsorption affinity  $b$  is sufficiently small.

**NON-DIMENSIONALIZATION OF THE MODEL**

The dimensionless variables and parameters are defined and listed in Table 1. Then the resulting dimensionless equations in terms of the dimensionless variables and parameters are as follows:

**Mass Balance in the Bed:**

$$\frac{\partial y_b}{\partial \tau} = \psi \theta \frac{1}{Pe} \frac{\partial^2 y_b}{\partial x^2} - \psi \theta \frac{\partial y_b}{\partial x} - 3\psi \zeta (y_b - y_s) \tag{4a}$$

$$\text{at } \tau=0, \quad y_b=0 \tag{4b}$$

$$\text{at } x=0, \quad \left[ \frac{\partial y_b}{\partial x} \right]_{x=0} = -Pe (y_b|_{x=0} - y_b|_{x=0'}) = -Pe (1 - y_b|_{x=0'}) \tag{4c}$$

$$\text{at } x=1, \quad \frac{\partial y_b}{\partial x} = 0 \tag{4d}$$

**Mass Balance in the Particle:**

$$\frac{\partial y_\mu}{\partial \tau} = \left( \frac{\partial^2 y_\mu}{\partial \eta^2} + \frac{2 \partial y_\mu}{\eta \partial \eta} \right) \tag{5a}$$

**Table 1. Definition of dimensionless variables and parameters**

$\eta = \frac{r}{R};$	$x = \frac{Z}{L};$	$\tau = \frac{D_e t}{R^2};$	
$y_b = \frac{C_b}{C_0};$	$y_s = \frac{C_s}{C_0};$	$y_\mu = \frac{C_\mu}{C_{\mu 0}};$	$y_{\mu s} = \frac{C_{\mu s}}{C_{\mu 0}}$
$C_{\mu 0} = \frac{C_{\mu s} b C_0}{1 + b C_0};$	$Bi = \frac{k_f R}{D_e};$	$Pe = \frac{vL}{D_e/\epsilon_b}$	
Distribution parameter $\psi = \frac{1 - \epsilon_b (C_{\mu 0})}{\epsilon_b (C_0)}$			
Bed length parameter $\theta = \delta/\lambda\psi$ , where $\delta = \frac{R^2/D_e}{L/v}$			
Film resistance parameter $\xi = \frac{Bi}{C_{\mu 0}/C_0}$			

$$\text{at } \tau=0, \quad y_\mu=0 \tag{5b}$$

$$\text{at } \eta=0, \quad \frac{\partial y_\mu}{\partial \eta} = 0 \tag{5c}$$

$$\text{at } \eta=1, \quad \left[ \frac{\partial y_\mu}{\partial \eta} \right]_{\eta=1} = \xi (y_b - y_s) \tag{5d}$$

**Adsorption Isotherm:**

$$y_\mu|_{\eta=1} = \frac{(1 + b C_0) y_s}{1 + b C_0 y_s} \tag{6}$$

**LDF MODEL**

For adsorption in a spherical particle, the adsorption rate based on the LDF approximation has the following dimensionless form:

$$\frac{\partial \langle y_\mu \rangle}{\partial \tau} = k_d (y_\mu|_{\eta=1} - \langle y_\mu \rangle) = 3\zeta (y_b - y_s) \tag{7}$$

where  $k_d$  is the dimensionless intraparticle mass transfer coefficient and  $\langle y_\mu \rangle$  is the dimensionless mean solid-phase concentration, defined as

$$k_d = \frac{d \langle y_\mu \rangle / d \tau}{(y_\mu)_{\eta=1} - \langle y_\mu \rangle} \tag{8a}$$

$$\langle y_\mu \rangle = 3 \int_0^1 y_\mu \eta^2 d\eta \tag{8b}$$

Based on Eq. (8a),  $k_d$  can be obtained from the reference as follows:

From Do and Rice [1986]

$$k_d = 15 \tag{9a}$$

From Do and Mayfield [1987]

$$k_d = 9 + \frac{1.153(0.32)}{\tau^{0.68}} \tag{9b}$$

From Hsuen [2000]

$$k_d = 3.8776 + \frac{1.6926}{\sqrt{\tau}} \tag{9c}$$

From the analytical solution of Crank [1975] for the particle diffusion

$$k_d = \frac{\pi^2 \sum_{n=1}^{\infty} \exp(-n^2 \pi^2 \tau)}{\sum_{n=1}^{\infty} \frac{1}{n^2} \exp(-n^2 \pi^2 \tau)} \tag{9d}$$

Substituting Eq. (7) into Eq. (4a), we have the following mass balance equation in the bed, based on the LDF model:

$$\frac{\partial y_b}{\partial \tau} = \psi \theta \frac{1}{Pe} \frac{\partial^2 y_b}{\partial x^2} - \psi \theta \frac{\partial y_b}{\partial x} - \psi k_d (y_\mu|_{\eta=1} - \langle y_\mu \rangle) \tag{10}$$

**NUMERICAL SOLUTION USING THE ORTHOGONAL COLLOCATION**

Eqs. (4), (5), and (6) formulate a nonlinear boundary value problem, which could be solved numerically by orthogonal collocation. For LDF models, the mass balance equation of Eq. (4a) should be

replaced by Eq. (10). If  $M$  interior collocation points for the axial domain and  $N$  interior collocation points for the radial domain were selected, the original system of partial differential equations [Eqs. (4) and (5)] could be transformed into a system of  $(M+MN)$  ordinary differential equations of initial value type by means of the collocation analysis.

Examining LDF model of Eq. (10), the concentration in the solid phase should be computed as a function of the particle radius first by using Eqs. (5), and then the surface concentration and the mean concentration in Eq. (10) could be obtained. Hence, there is no benefit of the less computer time of the LDF model over the exact model when we employ orthogonal collocation. Note that all  $(M+MN)$  ordinary differential equations should be solved simultaneously in the orthogonal collocation, contrasted with the step-by-step solution of the finite difference. However, the orthogonal collocation usually requires less computer time and gives more stable solution than the finite difference for a given accuracy of the numerical computation. Thus, the orthogonal collocation could be useful enough to test the validity of the LDF model through the comparison of the LDF model with the exact model.

Eight interior collocation points ( $M$ ) for the axial domain and four interior collocation points ( $N$ ) for the radial domain were selected, respectively, to solve the mathematical model in the present study. With more numbers of collocation points (e.g.,  $M=13$  and  $N=10$ ), similar numerical results could be obtained. The built-in function "ODE15S.M" of MATLAB was used as the integration routine to solve the resulting initial value problem of the  $(M+MN)$  coupled ordinary differential equations

## RESULTS AND DISCUSSION

As defined by Eqs. (4) and Eqs. (5), the model in the present study is identical to the problem solved numerically by Raghavan and Ruthven [1983] except that they employed a linear isotherm instead of the Langmuir isotherm of the present study. The Langmuir isotherm will reduce to a linear isotherm when the value of the adsorption affinity  $b$  is sufficiently small. This provides a convenient

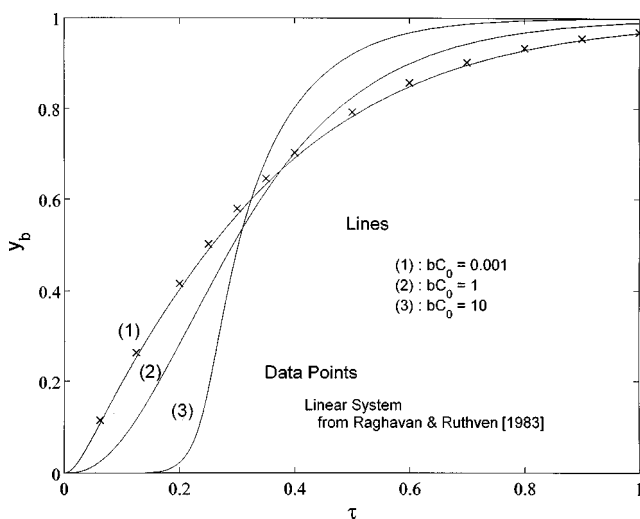


Fig. 1. Effect of adsorption affinity on the breakthrough curve in a short bed:  $\psi=10,000$ ,  $\theta=3$ ,  $Pe=5$ ,  $\xi=1,000$ .

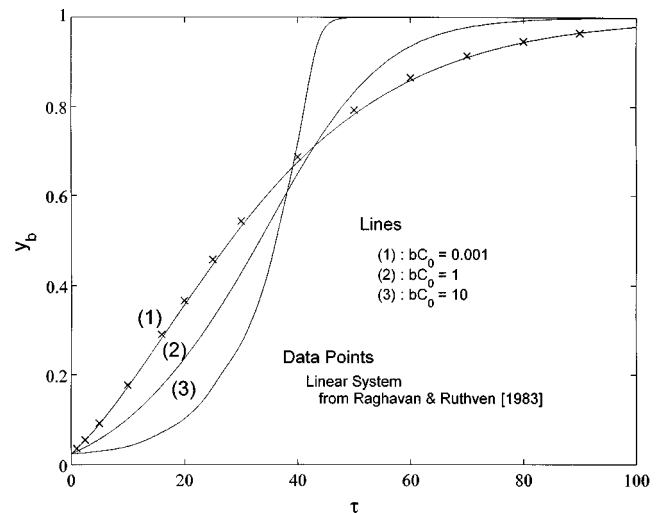


Fig. 2. Effect of adsorption affinity on the breakthrough curve in a long bed:  $\psi=10,000$ ,  $\theta=0.03$ ,  $Pe=10$ ,  $\xi=0.05$ .

check on the accuracy of the numerical computation of the model in the present study because the numerical solution of the linear version of the model has been reported in the reference [Raghavan and Ruthven, 1983; Chen and Hsu, 1987].

Fig. 1 and Fig. 2 show the orthogonal collocation solutions for representative sets of parameters. Fig. 1 is the result for a short column with high  $\xi$  (probably in the particle diffusion regime), while Fig. 2 is the result for a long column with small  $\xi$  (probably in the external film diffusion regime). The data points in both Figs. 1 and 2 are from Raghavan and Ruthven [1983] and curves are computed by the orthogonal collocation solutions in the present study. Comparing the breakthrough curves for  $1 \gg bC_0$  (i.e., for a linear system) with the data points in Figs. 1 and 2, we can conclude that the agreement between the numerical results from Raghavan and Ruthven [1983] and from the present study is excellent. When the adsorption affinity becomes larger, the breakthrough curve becomes

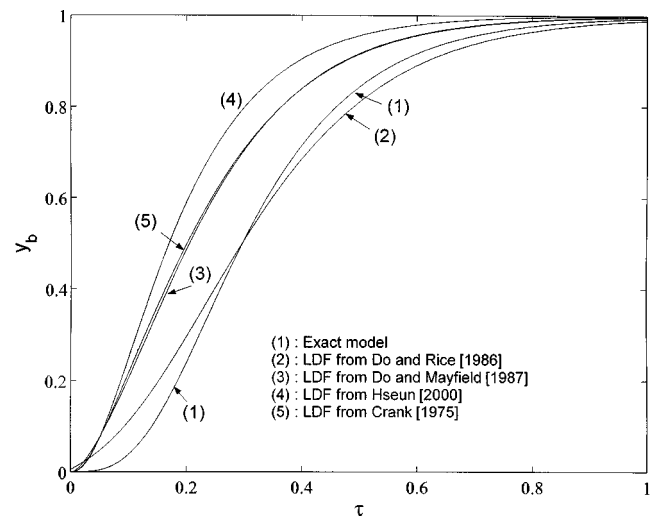


Fig. 3. Comparison of breakthrough curves in a short bed between the exact model and the LDF model:  $\psi=10,000$ ,  $\theta=3$ ,  $Pe=10$ ,  $\xi=1,000$ ,  $bC_0=1$ .

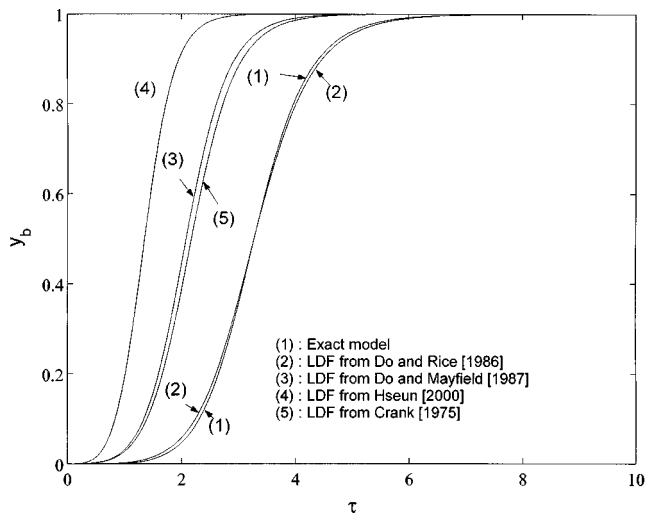


Fig. 4. Comparison of breakthrough curves in a medium bed between the exact model and the LDF model:  $\psi=10,000$ ,  $\theta=0.3$ ,  $Pe=10$ ,  $\xi=10$ ,  $bC_0=1$ .

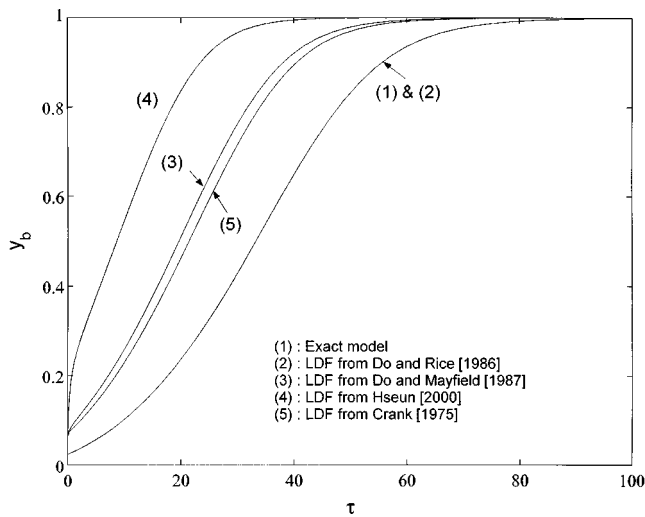


Fig. 5. Comparison of breakthrough curves in a long bed between the exact model and the LDF model:  $\psi=10,000$ ,  $\theta=0.03$ ,  $Pe=10$ ,  $\xi=0.05$ ,  $bC_0=1$ .

much steeper, as shown in Figs. 1 and 2.

Figs. 3, 4, and 5 show the breakthrough curves predicted by both the exact model and the LDF model for a short, a medium, and a long bed, respectively. Among four LDF models used in the present study, the model of Do and Rice [1986], which is based on the parabolic concentration profile in the particle, shows to be the best agreement with the exact model. For the shorter bed (i.e., for the larger value of the bed length parameter  $\theta$ ), there is some deviation between the exact model and the LDF model of Do and Rice. For the longer bed (i.e., for the smaller value of the bed length parameter  $\theta$ ), however, the agreement is seen to be excellent, noting in Fig. 5 that the breakthrough curves predicted by the model of Do and Rice and the exact model nearly coincide with each other. This is not surprising if we remember that the model of Do and Rice is based on the assumption of a symmetric intraparticle concentration pro-

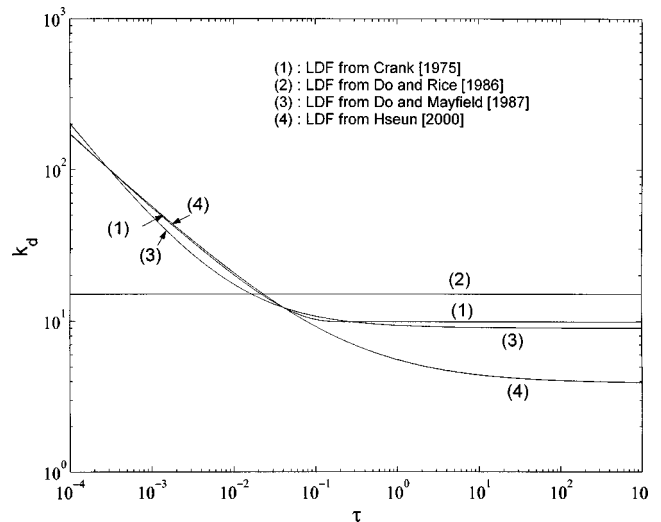


Fig. 6. Comparison of the dimensionless intraparticle mass transfer coefficients of various LDF models.

file, which can be practically attained in a sufficiently long bed.

The accuracy of the LDF model depends on that of the intraparticle mass transfer coefficient  $k_d$ . Fig. 6 shows the time dependence of the mass transfer coefficient. We can see in this figure that there are some discrepancies between the mass transfer coefficients from various LDF models. It has been known, since Gluckauf and Coates [1947], that the LDF model with  $k_d=15$  approximates the exact model very closely. The values of  $k_d$  from other LDF models except for the model of Do and Rice deviate largely from 15 in the range of  $0.1 < \tau$ , which is a practically important range for the breakthrough curves (note that there are also large deviations in the range of  $\tau < 0.1$ ). This is the reason why the breakthrough curves predicted from the LDF models deviate from the exact model more or less, depending on the magnitude of the deviation of  $k_d$  from 15, as shown in Figs. 3-5.

Figs. 7 and 8 show the comparison of the breakthrough curves predicted from the model of Do and Rice and the exact model: Fig.

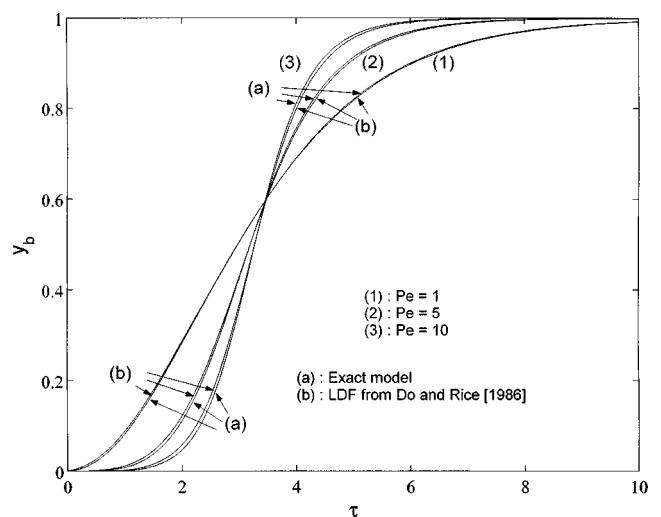


Fig. 7. Effect of  $\xi$  on the breakthrough:  $\psi=10,000$ ,  $\theta=0.3$ ,  $Pe=10$ ,  $bC_0=1$ .

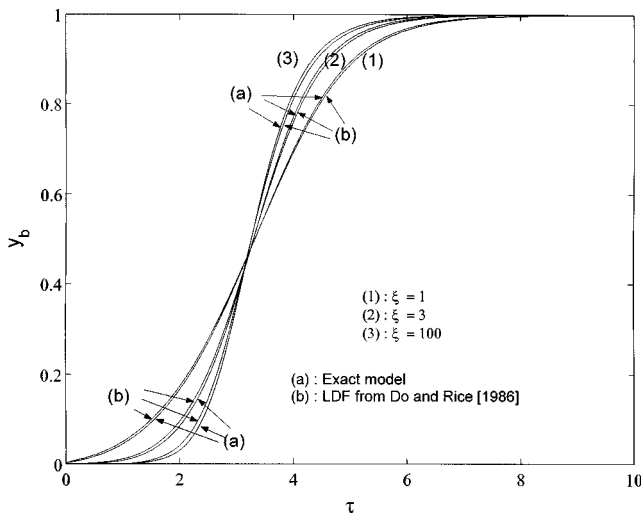


Fig. 8. Effect of  $\xi$  on the breakthrough:  $\psi=10,000$ ,  $\theta=0.3$ ,  $Pe=10$ ,  $bC_0=1$ .

7 for the effect of  $Pe$  and Fig. 8 for the effect of  $\xi$  on the breakthrough curve. As we can see in Fig. 7, the deviation of the LDF model based on the parabolic concentration profile from the exact model becomes smaller as  $Pe$  decreases. This is because the intraparticle diffusion resistance becomes relatively less important as  $Pe$  decreases. This argument is also true on the effect of  $\xi$ ; that is, the deviation of the LDF model from the exact model becomes smaller as  $\xi$  decreases. Thus, we can conclude that the LDF model based on the parabolic concentration profile approximates the exact model more closely as the intraparticle diffusion resistance becomes relatively less important compared to both the axial diffusion resistance and the external diffusion resistance.

### CONCLUSION

In the present study, we analyzed numerically the fixed bed adsorption kinetics using orthogonal collocation to test the validity of the simplified model based on the LDF approximation by comparison with the exact model.

Among four LDF models cited in the present study, the model from Do and Rice [1986], which is based on the parabolic concentration profile in the particle, shows to be best agreement with the exact model.

The LDF model based on the parabolic concentration profile deviates to some extent from the exact model in shorter bed. However, the deviation becomes negligible in a sufficiently long bed, in which the intraparticle concentration profile approaches a symmetric form.

As the intraparticle diffusion resistance becomes relatively less important compared to both the axial diffusion resistance and the external diffusion resistance, the LDF model based on the parabolic concentration profile approximates the exact model more closely.

### ACKNOWLEDGMENT

This work was supported by the Kyungnam University Research Fund, 2002.

### NOMENCLATURE

- $b$  : Langmuir isotherm parameter, defined by Eq. (3) [ $\text{cm}^3/\text{mol}$ ]  
 $Bi$  : Biot number, defined in Table 1  
 $C_b$  : concentration in the fluid phase [ $\text{mol}/\text{cm}^3$ ]  
 $C_0$  : intensity of step concentration at the inlet of bed [ $\text{mol}/\text{cm}^3$ ]  
 $C_s$  : concentration in the fluid phase at the particle surface [ $\text{mol}/\text{cm}^3$ ]  
 $C_\mu$  : concentration in the particle phase [ $\text{mol}/\text{cm}^3$ ]  
 $C_{\mu 0}$  : reference concentration, defined in Table 1 [ $\text{mol}/\text{cm}^3$ ]  
 $C_{\mu s}$  : Langmuir isotherm parameter, defined by Eq. (3) [ $\text{mol}/\text{cm}^3$ ]  
 $D_e$  : effective diffusivity, defined by Eq. (2a) [ $\text{cm}^2/\text{s}$ ]  
 $D_L$  : axial dispersion coefficient, defined by Eq. (1a) [ $\text{cm}^2/\text{s}$ ]  
 $k_d$  : dimensionless intraparticle mass transfer coefficient, defined by Eq. (8a)  
 $k_f$  : external mass transfer coefficient, defined by Eq. (2d) [ $\text{cm}/\text{s}$ ]  
 $L$  : bed length [ $\text{cm}$ ]  
 $M$  : number of interior collocation points in axial domain  
 $N$  : number of interior collocation points in radial domain  
 $Pe$  : Peclet number, defined in Table 1  
 $r$  : radial variable within the particle [ $\text{cm}$ ]  
 $R$  : radius of the spherical particle [ $\text{cm}$ ]  
 $t$  : time variable [ $\text{s}$ ]  
 $v$  : interstitial velocity of fluid in the bed [ $\text{cm}/\text{s}$ ]  
 $x$  : dimensionless axial variable in the bed, defined in Table 1  
 $y_b$  : dimensionless concentration in the fluid phase, defined in Table 1  
 $y_s$  : dimensionless concentration in the fluid phase at the particle surface, defined in Table 1  
 $y_\mu$  : dimensionless concentration in the particle phase, defined in Table 1  
 $\langle y_\mu \rangle$  : mean value of  $y_\mu$   
 $y_{\mu s}$  : dimensionless Langmuir isotherm parameter, defined in Table 1  
 $z$  : axial variable in the bed [ $\text{cm}$ ]

### Greek Letters

- $\varepsilon_b$  : void fraction of the bed  
 $\delta$  : ratio of time constants, defined in Table 1  
 $\eta$  : dimensionless radial variable within the particle, defined in Table 1  
 $\theta$  : dimensionless bed length parameter, defined in Table 1  
 $\tau$  : dimensionless time variable, defined in Table 1  
 $\xi$  : dimensionless film resistance parameter, defined in Table 1  
 $\psi$  : dimensionless distribution parameter, defined in Table 1

### REFERENCES

- Chatzopoulos, D. and Varma, A., "Aqueous-Phase Adsorption and Desorption of Toluene in Activated Carbon Fixed Beds: Experiments and Model," *Chem. Eng. Sci.*, **50**, 127 (1995).  
 Chen, T.-L. and Hsu, J. T., "Prediction of Breakthrough Curves by the Application of Fast Fourier Transform," *AIChE J.*, **33**, 1387 (1987).  
 Crank, J., "The Mathematics of Diffusion," 2nd Ed., Clarendon Press, Oxford (1975).

- Crittenden, J. C. and Weber, Jr., W. J., "Predictive Model for Design of Fixed-Bed Adsorbers: Parameter Estimation and Model Development," *J. Environ. Eng. Div. Amer. Soc. Civil Engrs.*, **104**(EE2), 185 (1978).
- Do, D. D. and Mayfield, P. L. J., "A New Simplified Model for Adsorption in a Single Particle," *AIChE J.*, **33**, 1397 (1987).
- Do, D. D. and Rice, R. G., "Validity of the Parabolic Profile Assumption in Adsorption Studies," *AIChE J.*, **32**, 149 (1986).
- Gluckauf, E. and Coates, J. J., "Theory of Chromatography. Part IV. The influences of Incomplete Equilibrium on the Front Boundary of Chromatograms and on the Effectiveness of Separation," *J. Chem. Soc.*, 1315 (1947).
- Hsuen, H. K., "An Improved LDF Approximation for Intraparticle Adsorption," *Chem. Eng. Sci.*, **55**, 3475 (2000).
- Kim, S. J., Cho, S. Y. and Kim, T. Y., "Adsorption of Chlorinated Volatile Organic Compounds in a Fixed Bed of Activated Carbon," *Korean J. Chem. Eng.*, **19**, 61 (2002).
- Lee, D. H. and Moon, H., "Adsorption Equilibrium of Heavy Metals on Natural Zeolites," *Korean J. Chem. Eng.*, **18**, 625 (2001).
- Moon, H., Lee, J. W. and Park, H. C., "Adsorption of Phenols in a Fixed-Bed Adsorber Charged with Polymeric Sorbents," *Korean J. Chem. Eng.*, **9**, 225 (1992).
- Raghavan, N. S. and Ruthven, D. M., "Numerical Simulation of a Fixed-Bed Adsorption Column by the Method of Orthogonal Collocation," *AIChE J.*, **29**, 922 (1983).
- Wehner, J. F. and Wilhelm, R. H., "Boundary Conditions of Flow Reactor," *Chem. Eng. Sci.*, **6**, 89 (1956).
- Xiu, G. H. and Li, P., "Prediction of Breakthrough Curves for Adsorption of Lead(II) on Activated Carbon Fibers in a Fixed Bed," *Carbon*, **38**, 975 (2000).
- Yun, J. H., "Unusual Adsorber Dynamics Due to S-Shaped Equilibrium Isotherm," *Korean J. Chem. Eng.*, **17**, 613 (2000).